



ELSEVIER

Journal of Contaminant Hydrology 58 (2002) 169–189

JOURNAL OF

Contaminant
Hydrology

www.elsevier.com/locate/jconhyd

Interaction between water flow and spatial distribution of microbial growth in a two-dimensional flow field in saturated porous media

Martin Thullner^{a,*}, Laurie Mauclaire^a, Martin H. Schroth^a,
Wolfgang Kinzelbach^b, Josef Zeyer^a

^a*Institute of Terrestrial Ecology, Swiss Federal Institute of Technology (ETH) Zurich, Grabenstrasse 3, CH-8952 Schlieren, Zurich, Switzerland*

^b*Institute of Hydromechanics and Water Resources Management, Swiss Federal Institute of Technology (ETH), Zurich, Switzerland*

Received 9 July 2001; received in revised form 31 January 2002; accepted 12 April 2002

Abstract

Bacterial growth and its interaction with water flow was investigated in a two-dimensional flow field in a saturated porous medium. A flow cell ($56 \times 44 \times 1$ cm) was filled with glass beads and operated under a continuous flow of a mineral medium containing nitrate as electron acceptor. A glucose solution was injected through an injection port, simulating a point source contamination. Visible light transmission was used to observe the distribution of the growing biomass and water flow during the experiment. At the end of the experiment (on day 31), porous medium samples were destructively collected and analyzed for abundance of total and active bacterial cells, bacterial cell volume and concentration of polysaccharides and proteins. Microbial growth was observed in two stripes along the length of the flow cell, starting at the glucose injection port, where highest biomass concentrations were obtained. The spatial distribution of biomass indicated that microbial activity was limited by transverse mixing between glucose and nitrate media, as only in the mixing zone between the media high biological activities were achieved. The ability of the biomass to change the flow pattern in the flow cell was observed, indicating that the biomass was locally reducing the hydraulic conductivity of the porous medium. This biologging effect became evident when the injection of the glucose solution was turned off and water flow still bypassed the area around the glucose injection port, preserving the flow pattern as it was during the injection of the glucose solution. As flow bypass was possible in this system, the average hydraulic properties of the flow cell were not affected by the produced biomass. Even in the vicinity of the injection port, the total

* Corresponding author. Present address: Laboratory of Geoenvironmental Science and Engineering, 1006 Bradfield Hall, Cornell University, Ithaca, NY 14853, USA. Tel.: +1-607-2553156; fax: +1-607-2558615.

E-mail address: martin.thullner@cornell.edu (M. Thullner).

volume of the bacterial cells remained below 0.01% of the pore space and was unlikely to be responsible for the bioclogging. However, the bacteria produced large amounts of extracellular polymeric substances (EPS), which likely caused the observed bioclogging effects.

© 2002 Elsevier Science B.V. All rights reserved.

Keywords: Bioclogging; Hydraulic conductivity; Biomass; Visualization; Transverse mixing

1. Introduction

Biodegradation is often a desired process for the remediation of aquifers contaminated by organic compounds (Anderson and Lovely, 1997). These contaminants may serve as a carbon source for microorganisms, and increased biomass production rates are possible given that suitable electron acceptors are present (Zarda et al., 1998; Bolliger et al., 2000). Transverse mixing between the contaminant and the electron acceptor was found to be an important process controlling degradation rates on the pore scale (e.g., Raje and Kapoor, 2000) as well as on the field scale (e.g., Thorton et al., 2001). Theoretical studies could identify dispersion as the dominating process for transverse mixing (Cirpka et al., 1999; Oya and Valocchi, 1998).

Reduction of hydraulic conductivity and porosity of a saturated porous medium due to microbial growth, hereafter referred to as bioclogging, has been observed under various conditions (Baveye et al., 1998). Bioclogging may influence the feasibility of bioremediation techniques in several ways. For example, microbial activity in contaminated parts of an aquifer can clog porous media and thus limit the availability of oxidants to microorganisms. Conversely, controlled clogging of an aquifer may be used to block preferential flow paths to produce a more homogeneous sweep (Lappan and Fogler, 1996), or to build up biobarriers that could be used to intensify contact between bacteria and contaminant, which may increase the success of remediation. For these reasons, it is necessary to investigate and understand interactions between biomass (bacteria and extracellular polymeric substances (EPS) produced by bacteria) and flow in porous media.

Several authors have reported on significant reduction of hydraulic conductivity due to bioclogging (Taylor and Jaffé, 1990a; Cunningham et al., 1991; Vandevivere and Baveye, 1992b; Brough et al., 1997; Johnston et al., 1997; Wu et al., 1997). All of these studies were performed in laboratory systems using one-dimensional flow fields (i.e., columns). Models for interpretation of these data exist (e.g., Taylor and Jaffé, 1990b), but they do not appear to reproduce reductions of hydraulic conductivity properly (Vandevivere et al., 1995). Model shortcomings were attributed to microorganisms growing in colonies, which influence the hydraulic conductivity differently than a biofilm, and to the lack of inter-pore connections in the models (Vandevivere et al., 1995). Microbial growth and its influence on hydraulic properties of microscopic pore networks was investigated by Dupin and McCarty (2000) and Kim and Fogler (2000). Dupin and McCarty (2000) observed a correlation between hydraulic conductivity and biological growth and morphology, Kim and Fogler (2000) also observed a decrease in hydraulic conductivity, which was only partially reversed under bacterial starving conditions. They attributed irreversible clogging effects to the gelation of the EPS, which makes the EPS more resistant to shear forces. In

studies by Taylor and Jaffé (1990b) and Sharp et al. (1999) it was shown that biomass is not only able to reduce hydraulic conductivity and porosity, but may also lead to an increased dispersivity of the porous medium.

As natural flow systems usually do not behave like one-dimensional systems, investigation of bioclogging in two- or three-dimensional systems is of considerable interest. In such systems clogged parts of the porous medium can be bypassed by water flow. This may produce effects that cannot be observed in quasi-one-dimensional systems, in which potential flow bypassing of clogged parts of the porous medium is difficult to resolve.

To demonstrate that observed clogging effects are caused by biomass, it is necessary to determine the presence of biomass in the porous medium. In previous studies different parameters were used to quantify biomass: bacterial carbon content (Taylor and Jaffé, 1990a) phospholipid content (Vandevivere and Baveye, 1992b) biofilm thickness Cunningham et al., 1991). To monitor biomass distribution, confocal laser scanning microscopy (DeLeo and Baveye, 1997), epifluorescent microscopy (Wu et al., 1997) and plate counting (Brough et al., 1997) have been employed. Except for direct visual measurements in Cunningham et al. (1991), all of these methods are destructive and thus can be performed only once at the end of the experiments. Furthermore, only one parameter was measured in each study to describe the biomass distribution, thus assuming that this parameter is characteristic for total biomass. However, since biomass composition depends on the growth conditions (Christensen and Characklis, 1990), one single parameter may not give sufficient information on biomass distribution in a porous medium. As not only the bacterial cells but also EPS are assumed to be responsible for bioclogging (Baveye et al., 1998), their presence must be quantified, too. In order to relate observed clogging effects to the presence of biomass, it may therefore be desirable to measure a set of different parameters to quantify the biomass distribution in porous media. In addition, to avoid the limitations of destructive methods, application of a non-invasive method during an experiment may also increase our understanding of microbial growth in porous media.

The goal of this study was to investigate the interaction between water flow and microbial growth in a two-dimensional flow field. In particular, we wanted to visualize water flow and biomass distribution for a simulated point source contamination. We performed an experiment in a flow cell filled with glass beads as a porous medium. To assess biomass distribution present in the porous medium, we measured changes in visible light transmission throughout the experiment. In addition, we used a color dye to visually observe flow patterns. Finally, upon termination of the experiment, we destructively sampled the porous medium and measured the number of total and active bacteria, bacteria cell volume and concentrations of polysaccharides and proteins.

2. Materials and methods

2.1. Growth medium and inoculum

Glass beads were used as a porous medium. The mineral medium consisted of KNO_3 , 51 mg/l; KH_2PO_4 , 5 mg/l; NH_4Cl , 63 mg/l; NaCl , 25 mg/l; $\text{MgCl}_2 \cdot 6\text{H}_2\text{O}$, 10 mg/l; $\text{CaCl}_2 \cdot 2\text{H}_2\text{O}$, 38 mg/l; KCl , 20 mg/l; and NaSO_4 , 5 mg/l dissolved in de-ionized water.

After autoclaving the medium at 120 °C, a sterile mixture of trace elements, vitamins, selenite–tungstate solution and NaHCO_3 solution was added and pH was adjusted to 7.5. The mineral medium was sparged with argon gas and then kept under argon atmosphere to reduce its nitrogen and oxygen gas content.

The inoculum was prepared 24 h before inoculation of the porous medium. For this purpose *Pseudomonas* strain PS⁺ (Deutsche Sammlung von Mikroorganismen und Zellkulturen No. 12877) was grown in 2 l of mineral medium with 1 g/l glucose as substrate and nitrate as electron acceptor on an orbital shaker at 30 °C.

2.2. Setup and operation of the flow cell

The experiment was conducted in a flow cell (Fig. 1; height: 56 cm; width: 44 cm; thickness: 1 cm) that consisted of two parallel polycarbonate plates mounted on an aluminum frame. In addition, two pairs of aluminum braces were used to stabilize the plates from the outside (not shown in Fig. 1). The bottom of the flow cell was first filled with 303 g coarse glass beads followed by 3865 g fine beads (all packed under saturated conditions) to achieve a total filling height of 55 cm. The coarse beads had a diameter of 1 mm and the fine beads a diameter of 0.4–0.6 mm. Both types of glass beads had a density of 2.5 kg/l. Due to pressure forces and the elasticity of the polycarbonate plates the total volume of the filled flow cell was increased from the calculated 2464 to 2720 ml (determined gravimetrically by filling the flow cell with water). Using this adjusted volume, the mass and density of the glass beads, the total porosity was calculated to be 0.38.

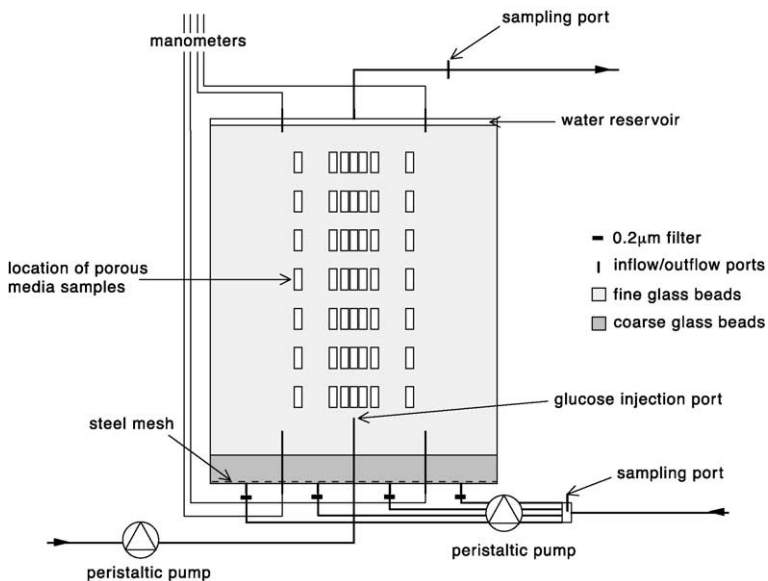


Fig. 1. Diagram of the experimental set-up (only flow cell and objects inside flow cell are drawn to scale). Aluminum frame and braces are not shown.

The flow cell was operated at a constant temperature of 22 °C in an upward-flow mode under water saturated conditions throughout the experiment. A peristaltic pump (IPN-4, Ismatec, Glattbrugg, Switzerland) was used to inject a mineral medium containing nitrate at four inflow ports at the bottom of the flow cell (Fig. 1). The pumping rate at each port was kept constant at 500 ml/day.

An additional injection port was placed 10 cm above the bottom and equidistant to the sides of the cell. At this port, glucose solution (1 g/l) was injected at a constant pumping rate of 40 ml/day using a peristaltic pump (IPC-16, Ismatec). The outflow port at the center on top of the flow cell was kept at constant hydraulic head. Manometers were placed close to the top and bottom of the flow cell within the fine beads pack (Fig. 1).

After packing of the flow cell and initiation of mineral medium flow, de-ionised water containing a color dye (Brilliant Blue FCF, Eriogluacine A, Fluka, Buchs, Switzerland) was injected at the glucose injection port and its distribution was monitored as a reference for glucose distribution during the experiment (see also Section 2.3). Furthermore, the breakthrough of chloride, injected at the four inflow ports with a total pumping rate of 2000 ml/day, was measured at the outflow to ensure the hydraulic functioning of the system and to determine the residence time of water in the flow cell.

Prior to starting the experiment, 2 l of the inoculum were injected via the inflow ports at the bottom of the flow cell using the same pumping rate as for the mineral medium. The experiment began when injection of glucose solution was initiated (day 1). On days 4, 9, 17 and 22, color tracer tests were performed by adding the color dye to the glucose to trace its distribution in the flow cell. An additional tracer tests was performed, for which the glucose injection was temporarily stopped (days 28–29). For this additional test, the glucose injection port was partially withdrawn and dyed de-ionized water was injected approximately 4 cm below the former glucose injection port at a flow rate of 40 ml/day. From day 29 onward, the experiment was performed as before this tracer test and ended on day 31.

2.3. Water flow and microbial growth visualization

Visible light transmission was used for water flow and biomass visualization. A light table was placed behind the flow cell (in an upright position). Light transmitted through the flow cell was recorded by a digital camera (JVC TK-C 1380E with Leica 1.2/12.5–75 mm lens) connected to a PC via a framegrabber (Leutron Picport, all from Leica Microsystems, Glattbrugg, Switzerland). Color pictures (red, green and blue channel (RGB), resolution 752 × 582 pixels) of the flow cell were taken and processed in two steps using Photoshop 5.5 (Adobe). The first step of picture processing was background subtraction with a background picture. In the second step, the RGB color pictures were separated by color channel, the red channel (maximum of contrast) was converted into a gray scale picture.

For visualization of the flow field, the injected fluids was dyed using Brilliant Blue FCF. Background pictures were taken just before dye injection. After background subtraction, the contrast of each single grey scale picture was maximised by linear amplification such that the darkest pixel(s) would attain a grey value of 255.

Biomass was visualized by taking a picture of the flow cell and subtracting a background picture, which was taken at the beginning of the experiment. All grey scale

pictures showing biomass had grey values ranging between 0 and 60. To increase the contrast, the grey value range was linearly amplified from 0 to 60 to the full range of 0–255 for each picture in identical fashion. To avoid interference between signals from the biomass and the color dye, pictures for biomass visualization were taken when no dye was present in the flow cell.

2.4. Water and porous medium sample collection

Water samples were collected once per day from inflow (2–3 ml/sample) and outflow (10 ml/sample) sampling ports. During the chloride tracer test, the sampling interval at the outflow sampling port was between 0.5 and 7 h.

On day 31 (end of the experiment), the flow cell was drained (flow rate approx. 1 l/h), placed into horizontal position and opened by removing the top plate. Forty-nine porous medium samples were collected (7 transects \times 7 samples per transect, see Fig. 1). Each porous medium sample of 3 cm³ in volume (3 \times 1 \times 1, approx. 5 g wet weight) was homogenized and divided into four sub-samples (2.0, 2.0, 0.5 and 0.5 g). The two 2-g sub-samples were immediately used for polysaccharide and protein quantification, while the two 0.5-g sub-samples were fixed for subsequent bacterial counts according to the method of Zarda et al. (1997).

2.5. Chemical and biological analyses

Water samples were analyzed for nitrate and chloride using a Dionex DX-100 ion chromatograph (Dionex, Sunnyvale, CA, USA), equipped with an electrical conductivity detector. All biological analysis were performed using nanopure-water and acid washed glass material. Results are averages of triplicates \pm standard error.

Total concentration of polysaccharides (EPS and bacteria) in the sampled porous medium were measured using the Dubois method (Dubois et al., 1956). Absorbance of light (wavelength 495 nm) was measured with a spectrometer (Uvicon, Kontron Instruments, Switzerland) against the reagent blank. Measured values were compared against fresh glucose solution of 0.0, 3.5, 7.0, 17.0, 28.0, and 35.0 μ g/ml water as standards.

Total concentration of proteins (EPS and bacteria) were measured using the Lowry method (Lowry et al., 1951). Absorbance of light (wavelength 750 nm) against the reagent blank was measured using the same spectrometer as previously mentioned. Measured absorbance values were compared against standards of 1, 2, 5, 10, 15, 20 and 25 mg/l bovine serum albumin (BSA).

Number and volume of total bacteria were investigated using DAPI staining (4',6-diamidino-2-phenylindole, Porter and Feig, 1980) according to the method of Zarda et al. (1997) combined with image analysis. Slides mounted with citifluor were examined at 400 \times magnification (Zeiss Plan-Neofluar oil) with a Zeiss Axiophot microscope fitted for epifluorescence with a 50 W high-pressure mercury bulb and filter set 02 (Zeiss, G 365, FT 395, LP 420). At least 400 bacteria per slide triplicate were manually counted. Bacterial volumes were measured by an image analysis system in five images per triplicate with up to 100 cells per image (Schönholzer et al., 1999). Cell volume was determined based on measurements of area and perimeter for each organism or bacterial aggregate.

After subsequent determination of fiberlength and fiberwidth, bacterial volumes were calculated (Analytical Vision, 1992; Russ, 1995).

To determine whether bacteria were metabolically active in the system, the number of ETS-active bacteria (i.e., bacteria with an active electron transport system) in porous medium samples was measured using 5-cyano-2,3-ditolylyl tetrazolium choride (CTC) staining (Rodriguez et al., 1992). Fresh samples were incubated for 3 h in the dark at room temperature with CTC solution (1.4 mg/ml). Samples were diluted with 0.1% pyrophosphate. Bacteria were detached from the glass beads using ultrasonification (Sonifer B-12, Branson sonic power, Danbury, CT, USA) (Mermillod-Blondin et al., 2001). Aliquots were spotted onto gelatin-coated slides. Slides mounted with citiflour were examined as previously described with the microscope fitted with filter set Hq Cy3 (AHF, Germany; G 546, FT 560, BP 575–640). At least 400 bacteria (10×40 fields) were counted per slide triplicate.

3. Results

3.1. Hydraulic and chemical data

Chloride breakthrough was measured at the beginning of the experiment to check the hydraulic functioning of the system and to determine the residence time of water in the flow cell and the longitudinal dispersivity of the porous medium. Measured chloride

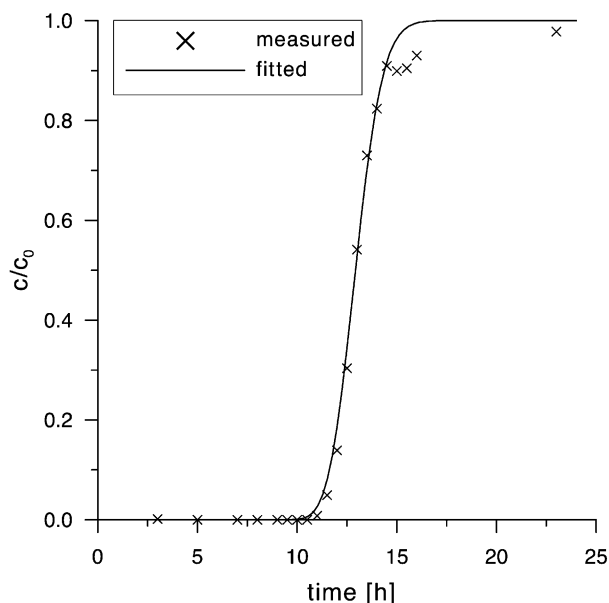


Fig. 2. Breakthrough of chloride at the outflow sampling port of the flow cell. Injection of concentration c_0 began at $t=0$.

concentration at the outflow sampling port increased smoothly between 10 and 15 h from background concentration to inflow concentration (Fig. 2). To compare the measured and theoretical breakthrough curves, flow was assumed to be one-dimensional within the cell. An analytical solution to solute transport of a conservative tracer in a one dimensional flow field taken from Bear (1972) was fitted to the measured data to determine values for pore water velocity u and the longitudinal dispersion coefficient D . For $u = 1.04$ m/day and $D = 0.002$ m²/day, the best fit was achieved (Fig. 2). The total residence time T of water in the entire flow cell (length: $x = 0.56$ cm, including the top zone filled with water only) is therefore $T = x/u = 0.54$ days. Given the total pumping rate of 2000 ml/day, this results in a computed average porosity of 0.39 for the porous medium, which is slightly higher than the porosity of 0.38 calculated from the weight of the glass beads. Assuming the relation $D = \alpha_L u$, we computed a longitudinal dispersivity $\alpha_L \approx 0.2$ cm.

Manometer measurements showed no changes in hydraulic head during the entire experiment (not shown). The head difference between the manometers at the top and the bottom of the flow cell was approximately 1 mm with no visible horizontal differences. Based on this value the hydraulic conductivity of the porous medium was estimated at 2.3×10^{-3} m/s.

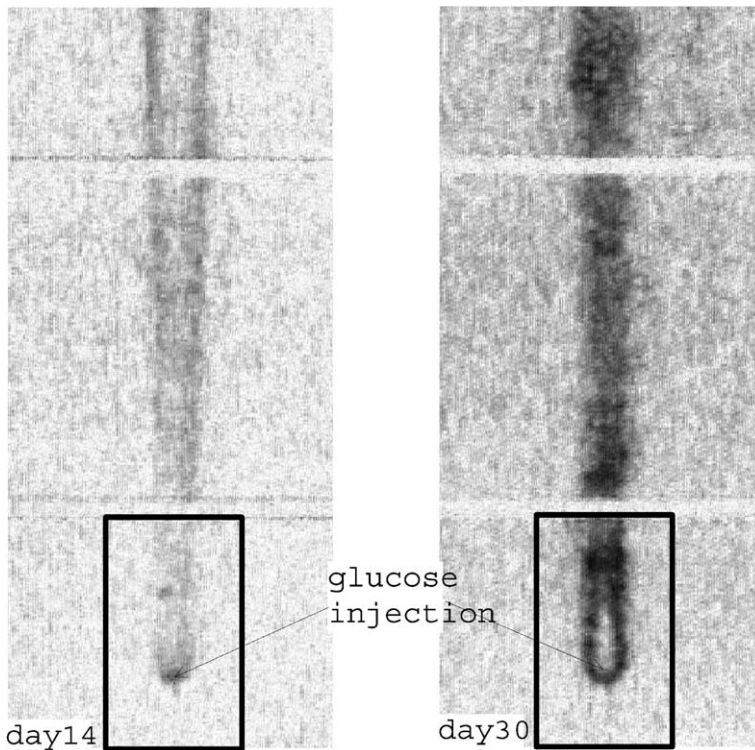
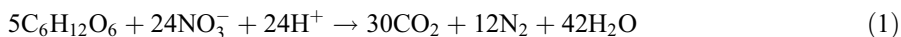


Fig. 3. Biomass (and partially gas) distribution in the flow cell. Pictures show a 46×20 cm area in the center of the flow cell; rectangles mark the observation zone used for detailed analyses.

Analysis of nitrate concentration at the inflow and outflow sampling ports indicated that nitrate consumption occurred in the flow cell. The inflow concentration was between 450 and 500 μM throughout the experiment, whereas the outflow concentration was generally smaller than the inflow concentration (not shown). Between days 17 and 27, the average nitrate concentration was approximately 450 μM at the inflow and 225 μM at the outflow. Using the total pumping rate of 2000 ml/day this corresponds to a nitrate consumption of approximately 0.45 mmol/day (50% of the injected amount). Assuming that the oxidation of glucose with nitrate is described by the equation



nitrate consumption of 0.45 mmol/day corresponds to a glucose oxidation of approximately 0.09 mmol/day or 42% of the amount of glucose injected per day. Between days 28 and 29 the glucose injection was stopped. During this period, the outflow concentration of nitrate exhibited an increase, approaching the inflow concentration (not shown).

3.2. Visual observations

About 1 week after the start of the flow cell experiment, an orange–brown colored substance was observed in the flow cell. This substance, assumed to be biomass, was initially located close to the glucose injection port, but later biomass was observed in a stripe pattern along the entire length of the flow cell starting near the glucose injection port (Fig. 3). Biomass was also found in the free water phase on top of the porous medium in the direct vicinity of the outflow port. About 3 weeks after the start of the experiment, gas bubbles could be observed in the upper regions of the flow cell, which interfered with the optical signals from the biomass. Subsequent measurement of the N_2 gas content in water collected from the outflow sampling port showed that the water was oversaturated with N_2 gas. Thus, the observed gas bubbles were attributed to N_2 gas production, showing that the argon sparging of the mineral medium was not sufficiently effective. However, the argon sparging seemed to reduce the N_2 gas content of the mineral medium at least partly as we

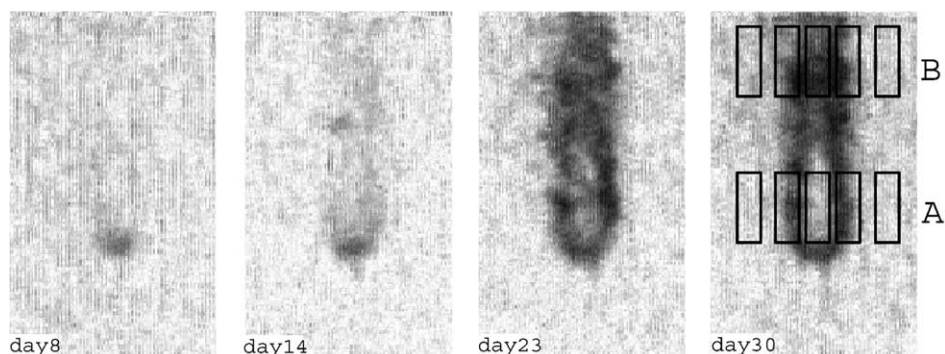


Fig. 4. Biomass distribution in a 14.5×8.5 cm observation zone around the glucose injection port. Rectangles show the position of the porous media sampling point of transects A and B in this zone.

observed no gas bubbles (but high amounts of biomass) in a zone close to the glucose injection port. Therefore, the results described below will focus on this observation zone, indicated by the rectangles in Fig. 3.

Within the observation zone the optical signals were attributed to biomass only. Pictures of visible light transmission indicate that during the experiment the biomass increased significantly, developing in a U- to ring-shaped pattern with its origin directly below the glucose injection port (Fig. 4). From the picture taken at day 30, we extracted the pixel values along the transects A and B. In Fig. 5, these values are shown as averages for the height (3 cm) of the transects. For transect A, a double peak pattern is clearly visible, whereas data for transect B show only a slight tendency to exhibit this double peak pattern. When comparing these data to the average pixel values for the area of the individual porous medium sampling points, the double peak pattern for transect A is much less pronounced, and for transect B only a single peak in the middle of the transect remains.

The color tracer tests with dyed glucose solution showed no significant changes in the distribution of the glucose solution throughout the experiment (Fig. 6). The pixel values along the center line were slightly more scattered towards the end of the experiment, but these effects were not pronounced enough to be considered significant. Data shown in Fig. 6 represent the quasi steady-state distribution of the glucose at the end of each tracer test, but also observations during the early stages of these tracer tests showed no changes in the flow of the glucose solution (data not shown). Conversely, during the color tracer test with dyed de-ionized water on days 28–29 (injected via the partially withdrawn glucose injection port), an influence of the biomass on the flow field could be observed (Fig. 7).

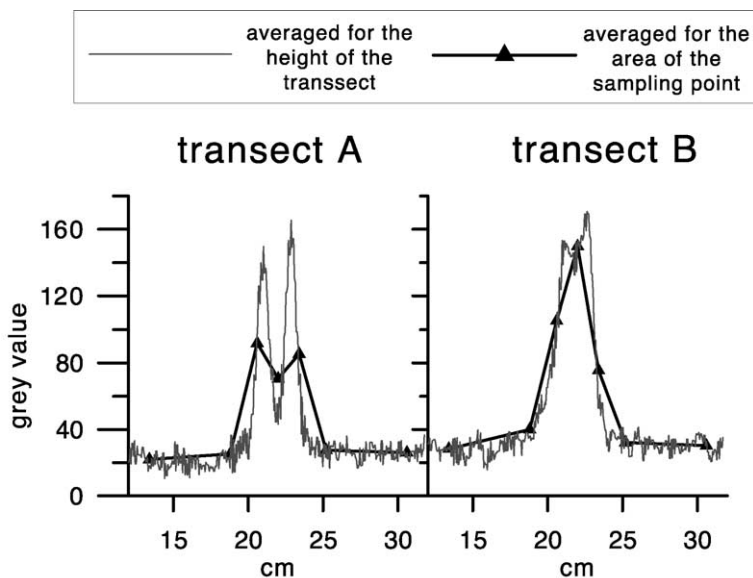


Fig. 5. Pixel values for transects A and B obtained by picture analysis. x-Axes show distance to left border of flow cell.

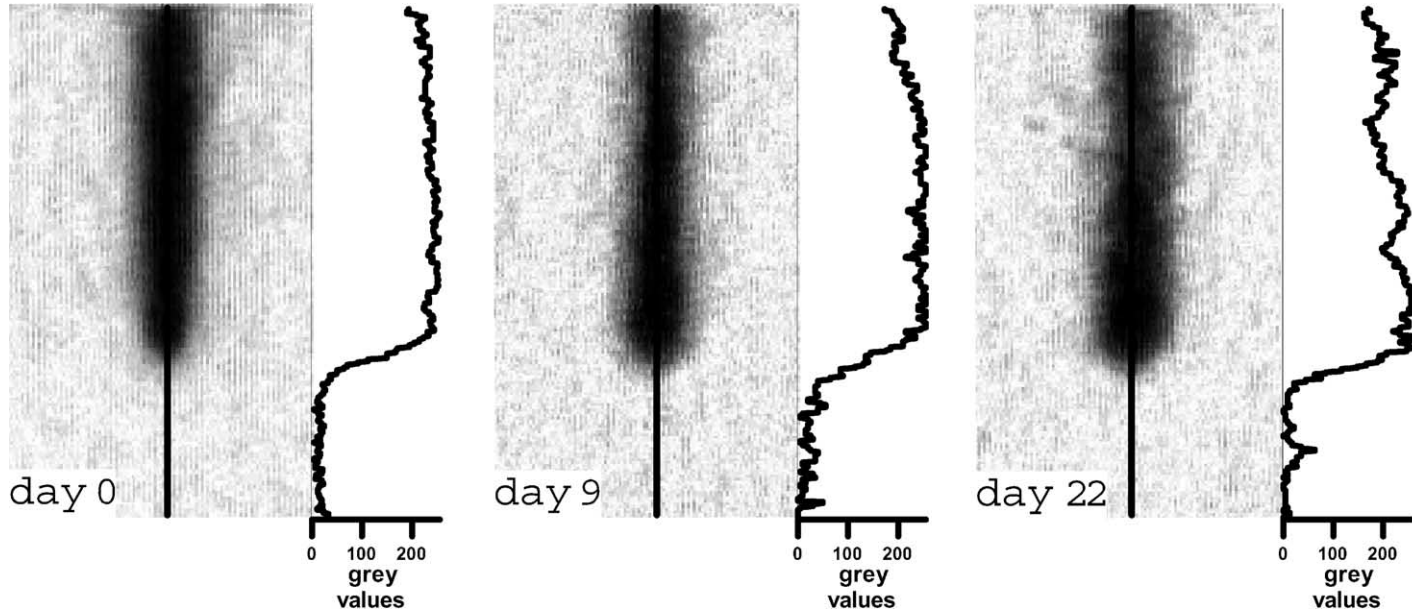


Fig. 6. Distribution of dyed solution injected at the glucose injection port before the experiment (day 0) and on selected days. Pictures were taken 1 day after injection of color dye was started. Grey values show pixel values along the black line in the center of the observation zone.

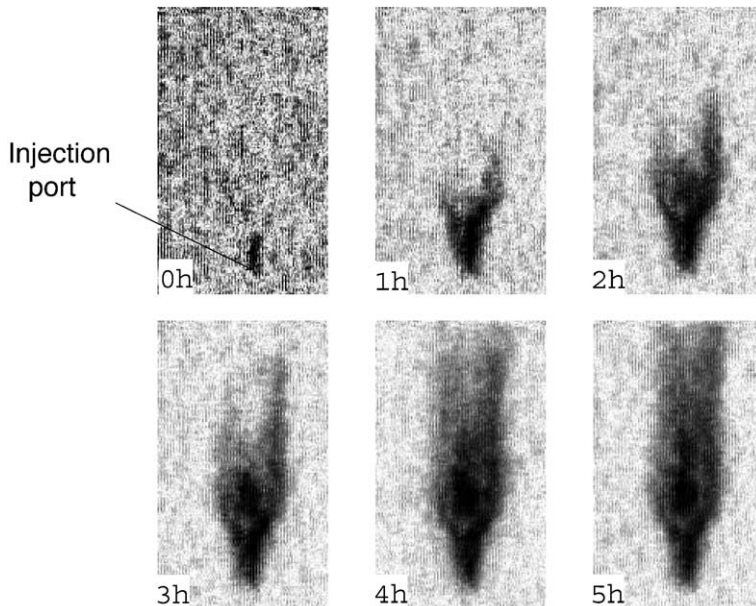


Fig. 7. Water flow surrounding the zone clogged by the biomass. Glucose injection was turned off and dyed water was injected via the partially withdrawn glucose injection port, starting at day 28. Legends show time after the start of color dye injection.

The flow of the dyed water tended to surround the area containing the biomass (note that Figs. 4, 6 and 7) show the same area of the flow cell), but this clogging effect was not strong enough to prevent dyed water from penetrating also the clogged area. Nevertheless, the flow pattern of the dyed water indicated that the biomass increased the flow resistance of the porous medium in that region.

3.3. Biological analyses

At the end of the experiment, porous medium samples were collected and analyzed for total number of bacteria, number of active bacteria, concentration of polysaccharides, and concentration of proteins. Results of these analyses show a strong variability of measured parameters along the transects (Fig. 8). All measured parameters show a two-stripe shaped growth zone in the center of the flow cell with highest values found in direct vicinity of the glucose injection port. Highest measured bacterial numbers were 190×10^6 cells/g beads for total bacteria and 17×10^6 cells/g beads for active bacteria, maximum concentrations were $29 \mu\text{g/g}$ beads for polysaccharides and $53 \mu\text{g/g}$ beads for proteins.

In addition, Fig. 9 shows the results for the two transects, A and B, located close to the glucose injection port. Results for transect A show a double peaked pattern for all measured parameters. For transect B, concentration of polysaccharides and to some extent concentration of proteins generate only a single peak in the middle of the transect. Total and active bacteria numbers exhibit a double peak pattern.

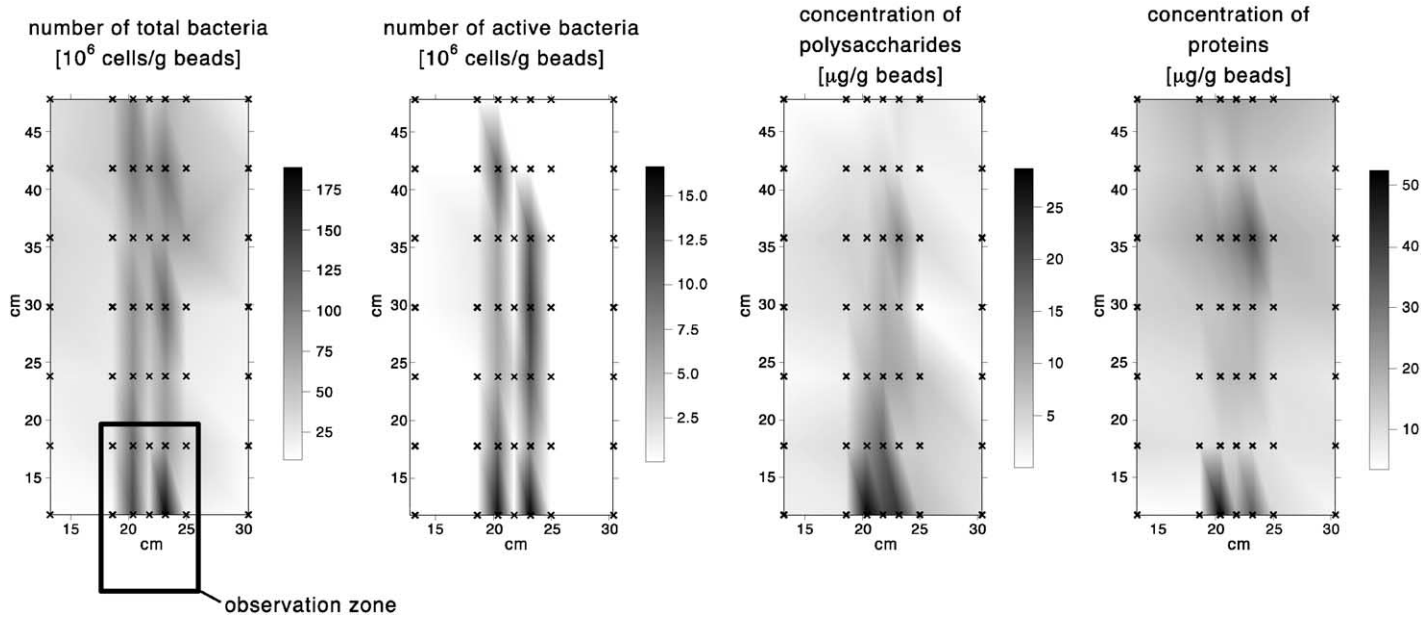


Fig. 8. Linear interpolation of measured biological parameters for all transects. Coordinates are relative to the lower left corner of the flow cell, “ × ” indicate the center of the individual sampling area.

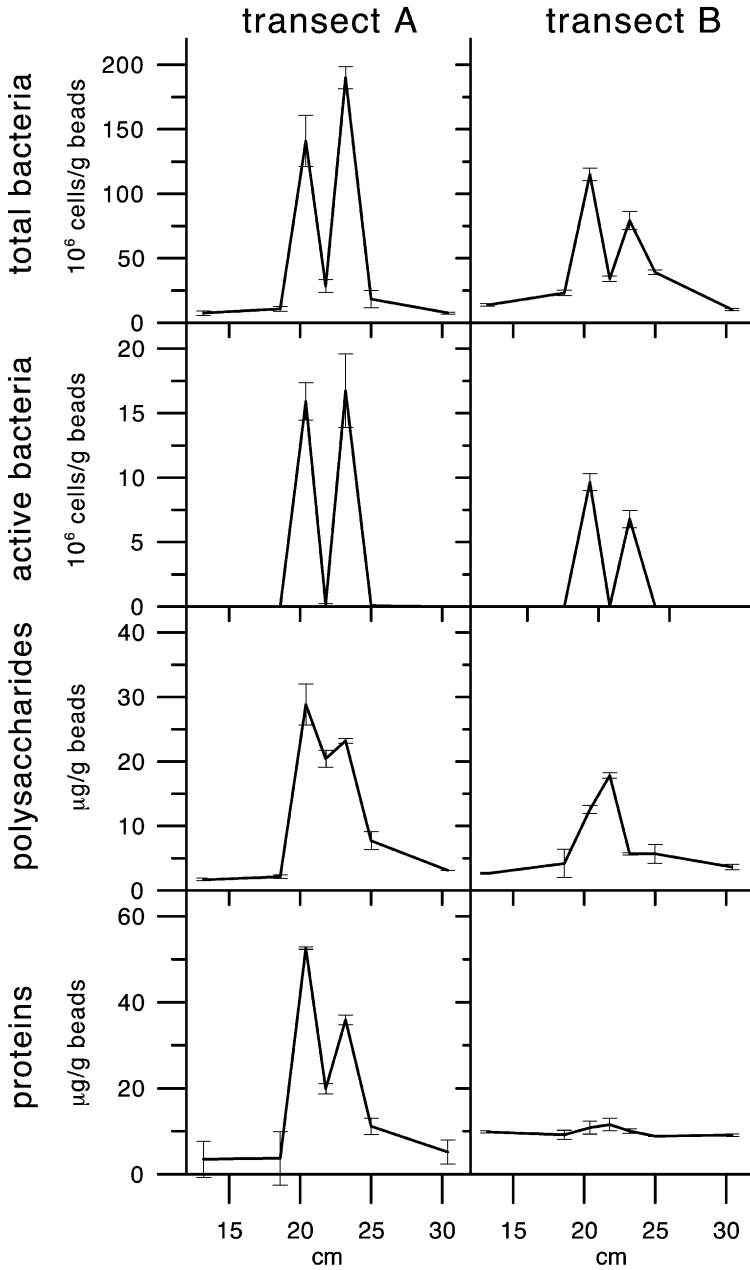


Fig. 9. Measured biological parameters for transects A and B. x-Axes show distance to left border of flow cell.

The average volume per bacterial cell was determined to be $0.082 \pm 0.006 \mu\text{m}^3$. Using average volume per bacterial cell, porosity, glass bead density and total number of bacteria, we calculated the volume fraction of the pore space occupied by bacteria to be less than 0.01%.

4. Discussion

Results from the chloride tracer test showed that the porous medium pack was highly homogeneous. Only a small discrepancy between measured and fitted chloride concentration towards the end of the breakthrough curve was observed, which we were unable to attribute to a specific cause. The computed dispersivity $\alpha_L \approx 0.2$ cm was slightly smaller than the value of 0.43 cm found by Sharp et al. (1999) for a similar system, supporting the assumption that our packing was highly homogeneous. Therefore, dispersive mixing between mineral medium and glucose solution affected the media's distribution only slightly. The fact that the nitrate concentration at the outflow approached the inflow concentration during the break in glucose injection indicates that nitrate consumption was coupled to glucose oxidation, suggesting a microbially mediated processes.

The distribution of the biomass was strongly influenced by the boundary conditions determining the flow field in the flow cell (Fig. 3). This was caused by the separate injection of electron donor (glucose) and acceptor (nitrate). Only where water from both origins mixed, microbial growth was possible. Thus, microbial growth was generally limited to a zone in the center of the flow cell starting from the glucose injection port upward. Biomass production occurred initially (days 8–14) in all parts of this zone, indicating that at least to a certain extent mixing took place. During the experiment, biomass production shifted to the boundary of this growth zone (Fig. 4). This may be explained by a consumption of the nitrate by the bacteria located at the boundary of the growth zone, which resulted in nitrate depletion in internal regions of the growth zone. Another plausible explanation is that clogging of the pores reduced mixing of water containing nitrate and water containing glucose.

The lack of changes in the spatial distribution of the glucose solution (Fig. 6) indicated that the produced biomass did not significantly affect the initial flow field during the experiment, as long as the flow boundary conditions (represented by the position of the injection and inflow ports and their flow rates) were not modified. Throughout the entire experiment the glucose was migrating between the two stripes of microbial growth. However, it was possible to show an influence of the biomass on the flow field when the boundary conditions for the flow were modified by changing the position of the glucose injection port (Fig. 7). This clearly indicated that biomass was generally able to influence the hydraulic properties of a porous medium and bioclogging took place as previously reported by several authors (e.g., Taylor and Jaffé, 1990a; Vandevivere and Baveye, 1992b). In case of a two-dimensional flow-field, as in the present experiment, bioclogging had a stabilizing effect on the flow field. This means that the initial flow field was not changed due to bioclogging but the flow pattern defined by the initial flow boundary conditions was preserved even when these flow boundary conditions were changed.

In a similar study, Kildsgaard (1999) also investigated bioclogging in a two-dimensional flow field, but they injected the electron donor and acceptor together at the same injection port and clogging effects in their study were different from the results of our study. In Kildsgaard (1999), the buildup of a clogged zone in the flow path of the nutrients was observed, forcing the water to bypass this zone while the flow boundary conditions were not changed. The differences between the results of the current study and the study of Kildsgaard (1999) show that the occurrence of bioclogging is highly dependent on the method of nutrient addition. In contaminated aquifers electron donor and acceptor are often from different sources (e.g., for the case of a point source petroleum hydrocarbon contamination or for the case of an engineered remediation system where the electron acceptor is injected as a point source). A laboratory system that uses separate injection systems for electron donor and acceptor, as was the case in this study, is therefore better suited to simulate a point source contamination or an engineered system, as mentioned above.

Although the hydraulic parameters were not measured locally, data shown in Fig. 7 suggest that the clogged part of the system was less permeable to flow. As indicated by the tracer test on days 28 and 29 (when no glucose but dyed water was injected), the clogging must be attributed to the accumulation of biomass in the pore space. Nevertheless, dyed water eventually entered this clogged part, which indicates that the reduction in hydraulic conductivity did not reach the extent reported elsewhere for column experiments. Reduction of hydraulic conductivity of more than three orders of magnitude, as observed, e.g. in experiments of Taylor and Jaffé (1990a) and Vandevivere and Baveye (1992b), should have nearly completely prevented dyed water from entering the clogged part of the flow cell. Conversely, flow bypass of a clogged zone, which can only take place in multi-dimensional flow fields, appears to play an important role for flow in considerably clogged porous media. Due to the possibility of flow bypass, the hydraulic conductivity of the entire flow cell remained essentially constant, showing that clogging can take place in a part of a multi-dimensional flow system without influencing the properties of the system on a larger scale.

The analysis of biological parameters at the end of the experiment showed that the biomass was mainly located in a growth zone, divided into two stripes, in the center of the flow cell (Fig. 8). This agrees with results from picture analysis (Fig. 3). Focusing on transects A and B, a comparison between the original pixel values and the average pixel value, which corresponds to a sample (Fig. 5), shows that the pattern observed by the picture analysis could only partly be resolved by the porous medium sampling scheme. Therefore, a higher spatial resolution of the measured biological parameters would have been desirable. However, the sample size and number used in this study had to be a compromise between a high spatial resolution and the minimum amount of sample material needed for the different analyses. Pixel values, averaged for the area of the sampling points (Fig. 5), agree well with the concentration of polysaccharides and proteins whereas the measured bacterial numbers show a slightly different pattern (Fig. 9). This suggests that EPS and not the bacteria were observed by picture analysis. The fact that the total volume of bacteria did not exceed a fraction of 0.01% of the porosity also supports this assumption.

To further determine, which fraction of the biomass was dominant, bacteria or EPS, we estimated the total amount of organic carbon and the amount of bacterial carbon for

transects A and B. We assumed that with the exception of polysaccharides and proteins other types of organic carbon can be neglected. Thus, the concentration of total organic carbon would be the sum of carbon in the polysaccharides and the proteins. From the molecular structure of polysaccharides and proteins (Stryer, 1990) the average carbon contents were assumed to be 0.40 ± 0.05 g C/g polysaccharides and 0.50 ± 0.20 g C/g proteins. Fig. 10 shows that for transect A organic carbon concentration reached 30–40 $\mu\text{g/g}$ beads, and was much higher compared to transect B with maximum concentration of approximately 10 $\mu\text{g/g}$ beads. For the calculation of bacterial carbon, the average carbon content per volume of the bacteria was an important variable. Values for this conversion factor published in literature (reviewed in Fry, 1990) vary between 0.05 and 0.65 mg C/cm³ bacterial cells with most of the values being between 0.05 and 0.35 g C/cm³. Therefore, we used an estimate of 0.20 ± 0.15 g C/cm³ bacterial cells, which resulted in a high uncertainty associated with the bacterial carbon concentration. Results of these calculations showed that bacterial carbon concentration did not exceed 4 $\mu\text{g/g}$ beads (Fig. 10) and the fraction of bacterial carbon in the total organic carbon is < 10% for most of the sampling points and with an average of approximately 5%, again indicating that the bulk of the biomass is formed by EPS and not by bacteria, which agrees with findings in Bakke

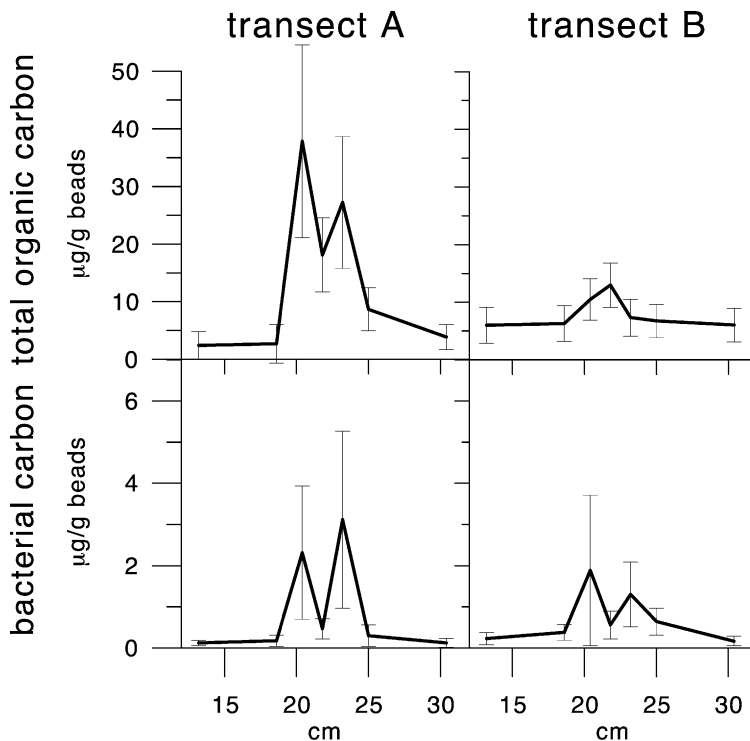


Fig. 10. Total organic carbon concentration and fraction of bacterial carbon on total organic carbon for transects A and B. x-Axes show distance to left border of flow cell.

et al. (1984). In addition, these results support observations made by Vandevivere and Baveye (1992a), who compared clogging efficiency of different bacterial strains in sand columns, showing that all strains produced similar amounts of bacterial mass, but only the EPS producing strain was able to clog the porous medium. Differences in the distribution of the bacteria and the EPS within the growth zone indicated that the bacteria and especially the active fraction of the bacteria were much more sensitive to the concentration of electron donor and acceptor as they could be found mainly in the mixing zone between the mineral medium and the glucose solution. Especially for transect B the EPS concentration exhibited a different distribution than the bacteria. A possible reason for this behaviour may be different growth or decay rates for bacteria and EPS (Kim and Fogler, 1999) or consumption of EPS by the bacteria (Walker and Pulkownik, 1973). Furthermore, the comparison between the total carbon concentration for transect A and B indicated that the total organic carbon had already decreased drastically between the two transects. This provides evidence that the area in direct vicinity of the glucose injection port was the zone of highest biological activity as suggested by data shown in Fig. 8 and by visual observations (Fig. 3).

To estimate the total amount of organic carbon in the porous medium at the end of the experiment we assumed that the biological activity was limited to a $45 \times 5 \times 1$ cm zone in the flow cell. Further assuming an organic carbon concentration of 40 $\mu\text{g/g}$ beads (approximate maximum from transect A) as a conservative estimate for all parts of this zone, the total organic carbon in the flow cell would only have been 13.7 mg or 3.5% of the total carbon injected as glucose. As only 42% of the injected glucose were oxidized with nitrate, not only nitrate but also glucose must have reached the outflow.

In addition, the buildup of biomass in the water reservoir close to the outflow was observed during the experiment. This indicates that mixing between the glucose and nitrate was the limiting process for microbial activity within the porous medium. Transverse mixing was therefore not only determining the spatial distribution of the biomass, but also the consumption of the glucose must be assumed to have taken place in the mixing zone only. This confirms findings of studies showing that the degradation of a contaminant plume is highly limited by transverse mixing (e.g., Cirpka et al., 1999; Thorton et al., 2001). This suggests that the size of the stripes, where biological activity took place, was correlated to the transversal dispersivity of the porous medium. As the chloride breakthrough curve could be used only to estimate the longitudinal dispersivity, the transversal dispersivity of the porous medium pack was not known. In case of a longer flow cell, it must be assumed that biomass would have continued to grow in the stripe pattern as observed in this study, until the glucose was completely consumed. From our observation there is no indication that clogging processes could become more relevant in that case.

Finally, it must be pointed out that the comparison between bacterial carbon and total organic carbon was done in terms of masses and not volumes. The biomass occupying the pore space was clearly visible towards the end of the experiment and this suggests that the total volume of biomass must have been orders of magnitude higher than the bacterial volume alone. This indicates that the density (expressed in mass of carbon per volume) must have been much smaller for the EPS than for the bacteria. Moreover, the small bacterial volume measured at the end of the experiment can not explain the observed

clogging effects, which confirms that the EPS and not the bacteria were responsible for the bioclogging in this experiment.

5. Conclusion

Results of this study show that for a two-dimensional flow field water flow and thus solute transport are dominating the spatial distribution of biomass in porous media. In addition, bioclogging effects in two-dimensional flow fields may drastically differ from observations made in one-dimensional flow fields. In a two-dimensional flow field bioclogging must not necessarily change a given flow pattern, but can also stabilize this flow pattern in case of changes in flow boundary conditions. Another difference between one- and two-dimensional flow fields is the effect of flow bypass of a clogged zone, which was observed in the present study. Due to flow bypass, clogging effects occurring locally did not change the hydraulic parameters of the entire system.

Data shown in this study demonstrate that it is necessary to determine both the distribution of bacteria and EPS to interpret bioclogging effects observed in an experiment. In particular, quantification of the bacterial carbon alone may drastically underestimate the amount of biomass present in the pore space. For a qualitative determination of growth and distribution of the total biomass, picture analysis has shown to be a suitable non-destructive method.

Acknowledgements

The authors would like to thank Toni Blunschli for constructing the flow cell and Annatina Zarda-Hess, Andreas Schürmann and Silvina Pombo (all from Swiss Federal Institute of Technology (ETH) Zurich, Switzerland) for support during the experiment. This study was funded by the Swiss Federal Institute of Technology (ETH) Zurich, Switzerland.

References

- Analytical Vision, I., 1992. Prism Image Analysis System, User's Manual. Analytical Vision Inc., Raleigh, NC, USA.
- Anderson, R.T., Lovely, D.R., 1997. Ecology and biogeochemistry of in situ groundwater bioremediation. *Adv. Microb. Ecol.* 15, 289–350.
- Bakke, R., Trulear, M.G., Robinson, J.A., Characklis, W.G., 1984. Activity of *pseudomonas aeruginosa* in biofilms: steady state. *Biotechnol. Bioeng.* 26, 1418–1424.
- Baveye, P., Vandevivere, P., Hoyle, B.L., DeLeo, P.C., Sanchez de Lozada, D., 1998. Environmental impact and mechanisms of the biological clogging of saturated soils and aquifer materials. *Crit. Rev. Environ. Sci. Technol.* 28 (2), 123–191.
- Bear, J., 1972. *Dynamics of Fluids in Porous Media*. Elsevier, New York.
- Bolliger, C., Schönholzer, F., Schroth, M.H., Hahn, D., Bernasconi, S.M., Zeyer, J., 2000. Characterizing intrinsic bioremediation in a petroleum hydrocarbon-contaminated aquifer by combined chemical, isotopic, and biological analyses. *Bioremediat. J.* 4 (4), 359–371.

- Brough, M.J., Al-Tabbaa, A., Martin, R.J., 1997. Active biofilm barriers for waste containment and bioremediation: laboratory assessment. Proc. Int. Symp. In Situ and On-site Bioremediation, New Orleans, USA, May 1997, vol. 4, pp. 233–238.
- Christensen, B.E., Charaklis, W.G., 1990. Physical and chemical properties of biofilms. In: Charaklis, W.G., Marshall, K.C. (Eds.), *Biofilms*. Wiley, New York, NY, USA. Chap. 4.
- Cirpka, O.A., Frind, E.O., Helmig, R., 1999. Numerical simulation of biodegradation controlled by transverse mixing. J. Contam. Hydrol. 40, 159–182.
- Cunningham, A.B., Charaklis, W.G., Abedeen, F., Crawford, D., 1991. Influence of biofilm accumulation on porous media hydrodynamics. Environ. Sci. Technol. (25), 1305–1311.
- DeLeo, P.C., Baveye, P., 1997. Factors affecting protozoan predation of bacteria clogging laboratory aquifer microcosms. Geomicrobiol. J. (14), 127–149.
- Dubois, M., Gilles, K.A., Hamilton, J.K., Rebers, P.A., Smith, F., 1956. Calorimetric method for determination of sugars and related substances. Anal. Chem. 28, 350.
- Dupin, H.J., McCarty, P.L., 2000. Impact of colony morphologies and disinfection on biological clogging in porous media. Environ. Sci. Technol. 34 (8), 1513–1520.
- Fry, J.C., 1990. Direct methods and biomass estimation. Methods Microbiol. 22, 41–85.
- Johnston, C.D., Rayner, J.L., De Zoysa, D.S., Ragusa, S.R., Trefry, M.G., Davis, G.B., 1997. Studies of bio-clogging for containment and remediation of organic contaminants. Proc. Int. Symp. In Situ and On-site Bioremediation, New Orleans, USA, May 1997, vol. 4, pp. 241–246.
- Kildsgaard, J., 1999. Experimental investigations and numerical simulations of the effect of biological growth on the hydraulic properties of porous media. Master thesis, Department of Hydrodynamics and Water Resources, Technical University of Denmark.
- Kim, D.-S., Fogler, H.S., 1999. The effect of expolymers on cell morphology and culturability of leuconostoc mesentroides during starvation. Appl. Microbiol. Biotechnol. 52, 839–844.
- Kim, D.-S., Fogler, H.S., 2000. Biomass evolution in porous media and its effects on permeability under starvation conditions. Biotechnol. Bioeng. 69 (1), 47–56.
- Lappan, R.E., Fogler, H.S., 1996. Reduction of porous media permeability from in situ leuconostoc mesentroides growth and dextran production. Biotechnol. Bioeng. 50, 6–15.
- Lowry, O.H., Rosenrough, N.J., Farr, A.L., Randall, J.R., 1951. Protein measurement with Folin phenol reagent. J. Biol. Chem. 193, 265–275.
- Mermillod-Blondin, F., Fauvet, G., Chalamet, A., Creuzé des Châtelliers, M., 2001. A comparison of two ultrasonic methods for detaching biofilms from natural substrata. Int. Rev. Hydrobiol. 83 (3), 349–360.
- Oya, S., Valocchi, A.J., 1998. Transport and biodegradation of solutes in stratified aquifers under enhanced in situ bioremediation conditions. Water Resour. Res. 34 (12), 3323–3334.
- Porter, K., Feig, Y., 1980. The use of DAPI for identifying and counting aquatic microflora. Limnol. Oceanogr. 25, 943–948.
- Raje, D.S., Kapoor, V., 2000. Experimental study of bimolecular reaction kinetics in porous media. Environ. Sci. Technol. 34, 1234–1239.
- Rodriguez, G.G., Phipps, D., Ishiguro, K., Ridway, H.F., 1992. Use of fluorescent redox probe for direct visualization of actively respiring bacteria. Appl. Environ. Microbiol. 58, 1801–1808.
- Russ, J.C., 1995. *The Image Processing Handbook*. CRC Press, Boca Raton, FL, USA.
- Schönholzer, F., Hahn, D., Zeyer, J., 1999. Origins and fate of fungi and bacteria in the gut of *Lumbricus terrestris* L. studied by image analysis. FEMS Microbiology Ecology 28, 235–248.
- Sharp, R.P., Cunningham, A.B., Komlos, J., Billmeyer, J., 1999. Observation of thick biofilm accumulation and structure in porous media and corresponding hydrodynamic and mass transfer effects. Water Sci. Technol. 39 (7), 195–201.
- Stryer, L., 1990. *Biochemie Spektrum-der-Wissenschaft-Verlagsgesellschaft*, Heidelberg, Germany.
- Taylor, S.W., Jaffé, P.R., 1990a. Biofilm growth and the related changes in the physical properties of a porous medium 1. experimental investigations. Water Resour. Res. 26 (9), 2153–2159.
- Taylor, S.W., Jaffé, P.R., 1990b. Biofilm growth and the related changes in the physical properties of a porous medium: 3. Dispersivity and model verification. Water Resour. Res. 26 (9), 2171–2180.
- Thorton, S.F., Quigley, S., Spence, M.J., Banwart, S.A., Botrell, S., Lerner, D.N., 2001. Processes controlling the

- distribution and natural attenuation of dissolved phenolic compounds in a deep sandstone aquifer. *J. Contam. Hydrol.* 53, 233–267.
- Vandevivere, P., Baveye, P., 1992a. Effect of bacterial extracellular polymers on the saturated hydraulic conductivity of sand columns. *Appl. Environ. Microbiol.* 58 (5), 1690–1698.
- Vandevivere, P., Baveye, P., 1992b. Saturated hydraulic conductivity reduction caused by aerobic bacteria in sand columns. *Soil Sci. Soc. Am. J.* 56 (1), 1–13.
- Vandevivere, P., Baveye, P., Sanchez de Lozada, D., DeLeo, P., 1995. Microbial clogging of saturated soils and aquifer materials: evaluation of mathematical models. *Water Resour. Res.* 31 (9), 2173–2180.
- Walker, G.J., Pulkownik, A., 1973. Degradation of dextrans by an α -1,6-glucan glucohydrolase from *streptococcus mitis*. *Carbohydr. Res.* 29, 1–14.
- Wu, J., Giu, S., Stahl, P., Zhang, R., 1997. Experimental study on the reduction of soil hydraulic conductivity by enhanced biomass growth. *Soil Sci.* 162 (10), 741–748.
- Zarda, B., Hahn, D., Chatzinotas, A., Schonhuber, W., Neef, A., Amann, R.I., Zeyer, J., 1997. Analysis of bacterial community structure in bulk soil by in situ hybridization. *Arch. Microbiol.* 168 (3), 185–192.
- Zarda, B., Mattison, G., Hess, A., Hahn, D., Höhener, P., Zeyer, J., 1998. Analysis of bacterial and protozoan communities in an aquifer contaminated with monoaromatic hydrocarbons. *FEMS Microbiol. Ecol.* 27, 141–152.